Journal of Applied Polymer Science

# Flexible and Flame Resistant Poly(lactic acid)/Organomontmorillonite Nanocomposites

**Wen Shyang Chow, Ee Lian Teoh**
School of Materials and Mineral Resources Engineering, Universiti Sains Malaysia, 14300 Penang, Malaysia
Correspondence to: W. S. Chow (E-mail: shyang@usm.my)

**ABSTRACT:** The PLA/OMMT nanocomposites were produced using a melt compounding technique with isopropylated triaryl phosphate ester flame retardant (FR; 10–30 parts per 100 resin). The flammability of the PLA/OMMT composites was evaluated with an Underwriter Laboratory (UL-94) vertical burning test, and their char morphology was studied using scanning electron microscopy (SEM). The thermal properties of the PLA/OMMT were characterized with a thermogravimetric analyzer (TGA) and a differential scanning calorimeter (DSC). The thermal analyses showed that adding FR reduced the decomposition onset temperature ($T_o$) of PLA/OMMT. Both PLA/OMMT/FR20 and PLA/OMMT/FR30 showed excellent flame retardant abilities, earning a V-0 rating during the UL-94 vertical burning test. A compact, coherent and continuous protective char layer was formed in the PLA/OMMT/FR nanocomposites. Additionally, the DSC results indicated that the flexibility of the PLA/OMMT composites increased after adding FR due to the FR-induced plasticization. The impact strength of PLA/OMMT was greatly increased by the addition of FR. Flexible PLA nanocomposites with high flame resistance were successfully produced. © 2014 Wiley Periodicals, Inc. J. Appl. Polym. Sci. **2015**, *132*, 41253.

**KEYWORDS:** clay; composites; flame retardance; thermal properties

Received 11 April 2014; accepted 2 July 2014
**DOI: 10.1002/app.41253**

## INTRODUCTION

The disposal of petroleum-based plastics and the restricted availability of petrochemical resources is a global concern. In recent years, biopolymers have been a focus of academic and industrial research in the context of sustainable development and reduced impact on the natural environment. Recent developments pertaining to the economical manufacturing of lactic acid from renewable agricultural resources (e.g., corn, potato, sugar beet, sugar cane) have made poly(lactic acid) (PLA) one of the most important biodegradable polymers. PLA offers good mechanical properties (i.e., high strength and modulus), a high degree of transparency, facile processability, good biocompatibility and excellent biodegradability. This material has a high tensile strength (50–70 MPa) and elastic modulus (3–4 GPa), allowing it to replace conventional polymers in numerous applications, such as packaging, extruded products, and thermoformed containers. Moreover, PLA exhibits similar processing characteristics to existing thermoplastic; therefore, PLA can be readily processed using existing production equipment. However, it should be noted that PLA still faces some challenges, e.g., inferior impact performance, low thermal stability and ignitability.[1–3]

Similar to other common petrochemical plastics, the ignitability of PLA and its tendency to drip during combustion limit its applications, especially in the electronic and electrical fields and in the automotive industry. The dripping of flaming melts is a particular problem that hinders the improvement of flame retardant thermoplastics. The flaming drips may lead to a rapidly spreading fire if highly flammable materials are available.[4] Therefore, improving the flame retardant properties of PLA has remained an important task. Polymer/clay nanocomposites have drawn extensive interest due to their improved mechanical, thermal, and flammability properties.[5] Although several studies have reported that polymer/clay nanocomposites can exhibit a decreased heat release rate (HRR), they are unable to impart self-extinguishing properties to the nanocomposites or pass the regulatory tests.[6]

It is known that the impact strength and toughness of PLA could be reduced by the addition of clay. Leu et al.[7] had reported that PLA/OMMT had displayed lower impact strength compare to the neat PLA. There is a need to improve the toughness and flexibility of PLA so that it can complete with commodity thermoplastics (e.g. polyethylene and polypropylene). Thus, various approaches including copolymerization, plasticization, and blending with elastomeric materials have been carried out to enhance the impact properties and toughness of PLA.[8–11] Recently, literatures showed that PLA can be toughened by maleated styrene-ethylene/butylenes-styrene,[7] poly(ethylene glycol),[11] maleic

**Table I.** Material Designations and Compositions of PLA Nanocomposites

| Material designation | Composition | | |
|---|---|---|---|
| | PLA (wt %) | OMMT (wt %) | FR (phr) |
| PLA | 100 | - | - |
| PLA/OMMT | 95 | 5 | - |
| PLA/OMMT/FR10 | 95 | 5 | 10 |
| PLA/OMMT/FR20 | 95 | 5 | 20 |
| PLA/OMMT/FR30 | 95 | 5 | 30 |

anhydride grafted ethylene-propylene rubber,[12] linear low density polyethylene,[13] poly(ethylene glycol)-functionalized polyhedral oligomeric silsesquioxane,[14] poly(ε-caprolactone) coated nano-titania particles,[15] and ultrafine full-vulcanized powdered rubber.[16]

In general, the combustion cycle of a polymer can be interrupted during a selected stage of the process, such as during heating, decomposition, ignition or flame spreading. Bourbigot and Fontaine[17] suggested three main approaches to reduce the flammability of PLA : chemical modification of the molecular structure, incorporation of flame retardants into the polymers and direct surface treatment of the PLA chain.

Although halogenated flame retardants efficiently quench flames and improve thermal stability, they negatively impact the environment. When halogenated substances are incinerated at high temperatures, they may produce toxic dioxins and furans; these compounds can cause cancer, birth defects, and neurological damage. Therefore, halogen-free flame retardants, such as metal oxides, metal hydroxides, phosphorus and melamine compounds, have attracted considerable attention in recent years.[18]

Inorganic phosphates, insoluble ammonium phosphate, organophosphates and phosphonates, chlorophosphates and phosphonates, bromophosphates, phosphine oxides, and red phosphorus are commonly used phosphorus-based flame retardants.[19,20] Triaryl phosphates are organophosphorus compounds that work well in oxygen-containing polymers, such as polyester, polyamide, poly(ethylene terephthalate) and poly(urethane).[21,22]

Wei et al.[23] reported that additive-type flame retardants are convenient for the manufacturing of materials and are used in PLA, and these materials are composed of phosphorus-containing, silicon-containing, and inorganic additives. Adding poly(9-oxa-10-(2,5-dihydro-xyphenyl) phospha-phenanthrene-10-oxide) phenylphosphonate to PLA leads to a V-0 rating during the UL-94 test.[23] Wang et al.[24] used ethyl phosphorodichloridate as a chain extender to synthesize poly(lactic acid)-containing phosphorus in the backbone (PPLA). The PPLA exhibited good flame retardant properties (V-0 in the UL-94 test with a Limiting Oxygen Index (LOI) value of 25%).

To the best of our knowledge, there have been no studies describing the flammability of PLA when using isopropylated triaryl phosphate ester as a flame retardant. This phosphorus-containing flame retardant (Reofos 50) is commonly used as a flame retardant for poly(vinyl chloride), polyurethanes, cellulosic resin and synthetic rubber and as a processing aid for engineering resins, such as modified poly(phenylene oxide) (PPO) and polycarbonate. This paper will elucidate the effects of a phosphorus-based flame retardant on the flammability, thermal and impact properties of PLA/OMMT nanocomposites.

## EXPERIMENTAL

### Materials

Poly(lactic acid) (PLA, Ingeo™ 3051D) was purchased from NatureWorks LLC, USA. This material has a specific gravity of 1.25 g/cm$^3$ and a melt flow index of 25 g/10 min (2.16 kg load, 210°C). The glass transition ($T_g$) and melting temperatures ($T_m$) of PLA are 60°C and 150°C, respectively. The organo-montmorillonite (OMMT, Nanomer 1.31PS) was supplied by Nanocor, Inc. This material exists as a white powder with its surface modified with 15 to 35 wt % of octadecylamine and 0.5 to 5 wt % of aminopropyltriethoxysilane. The mean dry particle size is less than 20 $\mu$m, and the bulk density is 200 to 500 kg/m$^3$. The phosphorus-based flame retardant (Reofos 50; FR) was provided by Chemtura Corporation, and has a phosphorus content of 8.3%. This clear liquid has a specific gravity of 1.17-1.18 g/cm$^3$ at 20°C. The liquid flame retardant possesses a viscosity of 53 to 64 cps at 25°C and contains 25 to 50% triphenyl phosphate (R=H), including more than 50% isopropylated triphenyl phosphate (R = isopropyl).

### Preparation of PLA Nanocomposites

Before melt compounding, the PLA pellets and OMMT powder were dried in an oven at 55°C for 24 h to remove any moisture. Subsequently, a predetermined amount of OMMT and FR were premixed manually at room temperature. The melt compounding was carried out with an internal mixer (Haake Rheomic Polydrive R 600/610) set at 170°C with a total mixing time of 10 min and a mixing speed of 50 rpm. To obtain PLA/OMMT/FR nanocomposites, PLA pellets were loaded into the internal mixer, and then the premixed OMMT/FR compound were added into the PLA after 5 min of mixing time. After melt mixing, the compounds were removed from the internal mixer and dehumidified at 55°C for 24 h before compression molding. The compression molding was carried out with a hydraulic press (Gotech, Taiwan) at 180°C. The specimens were compressed to a thickness of 3.2 mm for further testing. The materials composition and designation are presented in Table I.

### Characterization of PLA/OMMT/FR Nanocomposites

**Nanostructure Morphology Assessment.** TEM measurements were carried out with a transmission electron microscope (Carl Zeiss, model: Zeiss Libra 120 Plus) operating at an accelerating voltage of 120 kV. The specimens were prepared using an ultramicrotome (Boeckeler Instruments, model: PT-PC PowerTome). Ultra-thin sections of about 50 nm in thickness of the PLA nanocomposite specimen was cut with a diamond knife (Diatome, model: ultra 45°, Switzerland) at room temperature.

**Flammability Tests.** An Underwriters Laboratories (UL) 94 vertical burning test was performed according to ASTM D3801 with a HVUL Horizontal Vertical Flame Chamber (ATLAS Fire Science Product, Chicago). The test specimens were 120 mm ×

12.7 mm × 3.2 mm (length × width × thickness) and mounted vertically above a cotton patch. A 20 mm yellow-tipped blue flame was produced by adjusting the gas supply and air ports of the burner. The burner was tilted to 45 ± 5° perpendicular to the wide face of the specimen. The specimens were ignited at the bottom for 10 s. If the burning stopped, the flame was immediately reapplied for an additional 10 s. The times the flame persisted after the first ($t_1$) and second applications ($t_2$) were recorded. A total of two sets of specimens, with five specimens in each set, are prepared for each of the composition.

**Thermogravimetric Analysis (TGA).** Thermogravimetric analysis (TGA) was carried out to investigate the decomposition onset temperature ($T_o$), the temperature at the maximum degradation rate ($T_{max}$) and the char yield of the specimens (percentage). The $T_o$ refers to the onset decomposition temperature, and $T_{10}$ is defined as the temperature when 10% weight loss occurs, while $T_{50}$ indicates the temperature at which 50% weight loss occurs during thermal decomposition. $T_{max}$ denoted to the peak temperature at the maximum decomposition rate that determined from the DTG curves. The TGA tests were performed at 10°C/min under nitrogen. The samples weighed approximately 10 to 15 mg and were heated from 30 to 600°C.

**Differential Scanning Calorimetry (DSC).** Differential scanning calorimetry (DSC) was used to determine the glass transition temperature ($T_g$), melting temperature ($T_m$) and cold crystallization temperature ($T_{cc}$) of the PLA samples. The DSC analyses were performed with a Mettler-Toledo DSC1, USA, and were conducted under nitrogen using approximately 10 mg of sample sealed in aluminum pans. The samples were heated from 30–180°C at 10°C $min^{-1}$, held at 180°C for 1 min, and cooled to 30°C at 10°C $min^{-1}$. A second experiment was performed that was similar to the first.

**Microstructure Analysis.** A field emission electron microscope (FESEM, Supra 35VP, Carl Zeiss, Germany) was used to study the char morphology of the PLA surfaces. The surfaces were sputtered with gold before the FESEM examination. Energy dispersive X-ray Microanalysis (EDX 32, Genesis) was used to analyze the occurrence of elements in the char residue of the PLA composites.

**Impact Tests.** Charpy impact tests were carried out by using a pendulum-type testing machine (Type 5101, Zwick, Germany) in accordance to ASTM 6110-04. Five specimens were tested for each composition. The testing was performed with a pendulum of 7.5 J with a velocity of 3.84 m/s.

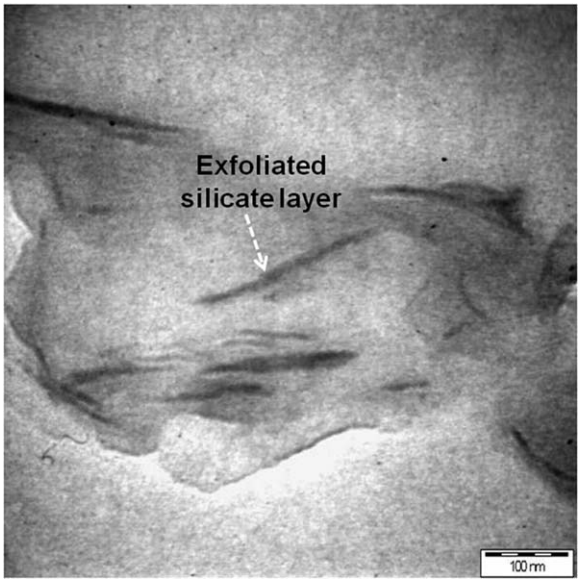


**Figure 1.** TEM images taken from the PLA/OMMT/FR nanocomposite.

## RESULTS AND DISCUSSION

### Morphology of PLA/OMMT/FR Nanocomposites

Figure 1 shows the TEM images taken from the PLA/OMMT/FR nanocomposite. The dark gray lines represented the thickness of individual clay layer. One may observe that the dispersibility of the OMMT layered silicate in the PLA is quite well and homogeneous, in the presence of FR. From the TEM micrograph, both intercalated and exfoliated OMMT were detected.

### UL-94 Vertical Burning Test

The UL-94 test is used to determine the relative flammability, dripping behavior and extinguishing characteristics of plastics employed as parts in devices and appliances.[25] Table II displays the UL-94 vertical burning test results of the neat PLA, PLA/OMMT and PLA/OMMT/FR composites. The pure PLA burned with vigorous dripping and bubbling when the flame was applied. The falling drips of PLA ignited the cotton indicator at the bottom of the holder clamp. Because the PLA could self-extinguish within 30 s after the first and second flame applications, a V-2 rating was achieved. The flowing and dripping

**Table II.** Effect of Varying the FR Loading on the Burning Behavior and the UL-94 Rating for the PLA Nanocomposites

| | After-flame time (s) | | | | |
|---|---|---|---|---|---|
| Materials designation | 1st flame application, $t_1$ | 2nd flame application, $t_2$ | Flame dripping | Cotton ignited | Rating |
| PLA | 6 ± 3 | 7 ± 2 | Yes | Yes | V-2 |
| PLA/OMMT | 12 ± 2 | 20 ± 3 | Yes | Yes | NR |
| PLA/OMMT/FR10 | 4 ± 2 | 3 ± 1 | Yes | Yes | V-2 |
| PLA/OMMT/FR20 | 3 ± 1 | 1 ± 1 | Yes | No | V-0 |
| PLA/OMMT/FR30 | 1 ± 1 | 1 ± 1 | Yes | No | V-0 |

Remarks: NR = no rating in UL-94 vertical burning test.

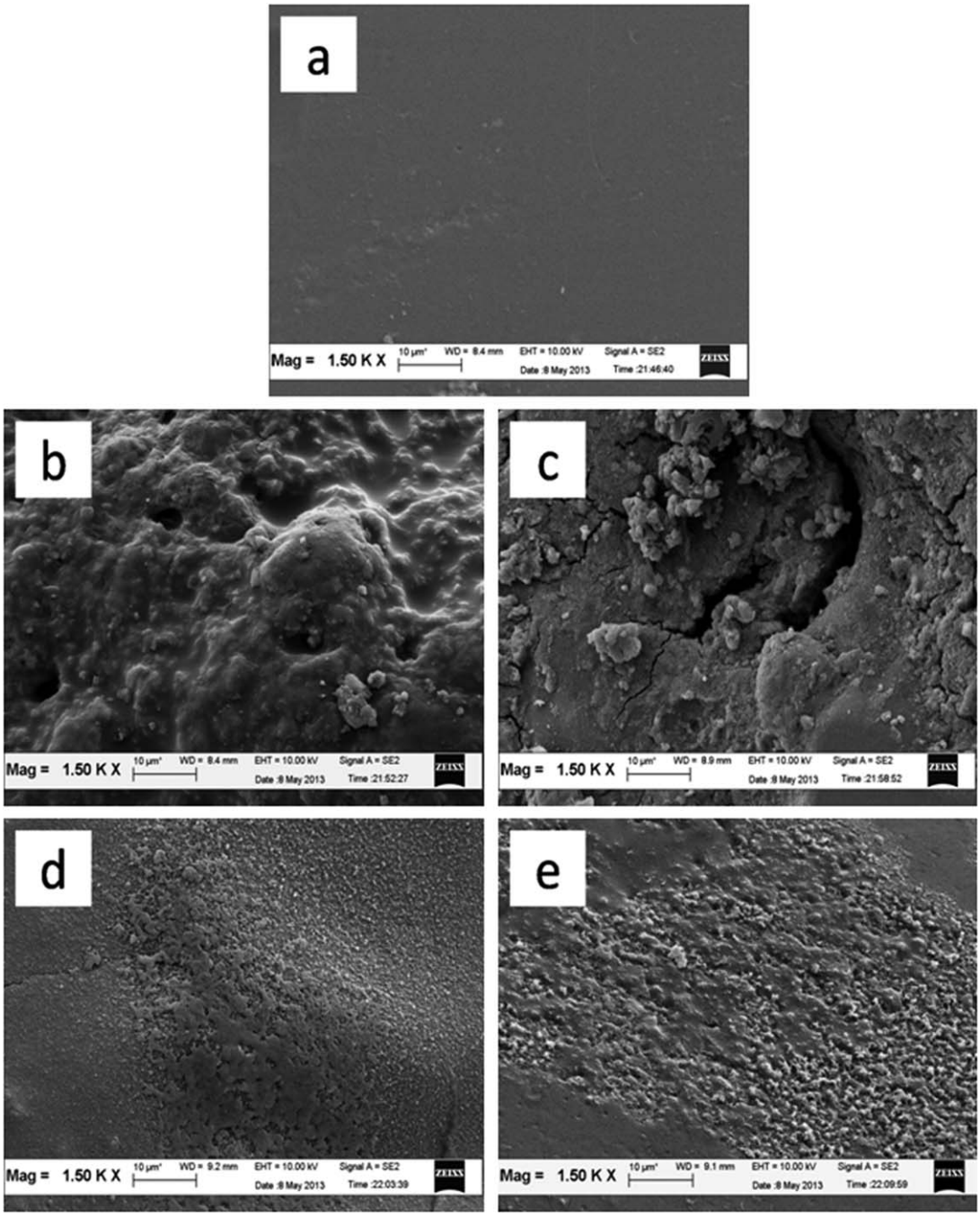


**Figure 2.** FESEM micrographs of the PLA composites after a UL-94 vertical burning test. (a) PLA, (b) PLA/OMMT, (c) PLA/OMMT/FR10, (d) PLA/OMMT/FR20, and (e) PLA/OMMT/FR30.

behavior of the PLA could remove heat from the surface when melting precedes ignition.[26] Because the specimens were mounted vertically during the burning test, the polymer that acted as the fuel was progressively withdrawn from the fire source, avoiding ignition and continuing fire growth. Therefore, PLA has good potential for qualifying via the UL-94 test.[27,28]

Note that there is no obvious improvement in the flame resistance of PLA by the incorporation of OMMT. According to Anna et al.[29] and Nazare et al.,[30] incorporating nanoclay increases the melt viscosity considerably, reducing the dripping and flowing behavior of the compound during ignition. Although the dripping tendency of PLA was reduced in the presence of the nanoclay, the falling drips still ignited the cotton, and the PLA was unable to self-extinguish. Because the mean total after-flame time exceeded 30 s for each specimen, the PLA/OMMT was assigned "no rating" in the UL-94 test. Studies have also revealed that nanoclay only improves the thermal stability of polymers by reducing the heat release rate (HRR) and slowing burning; these materials do not promote

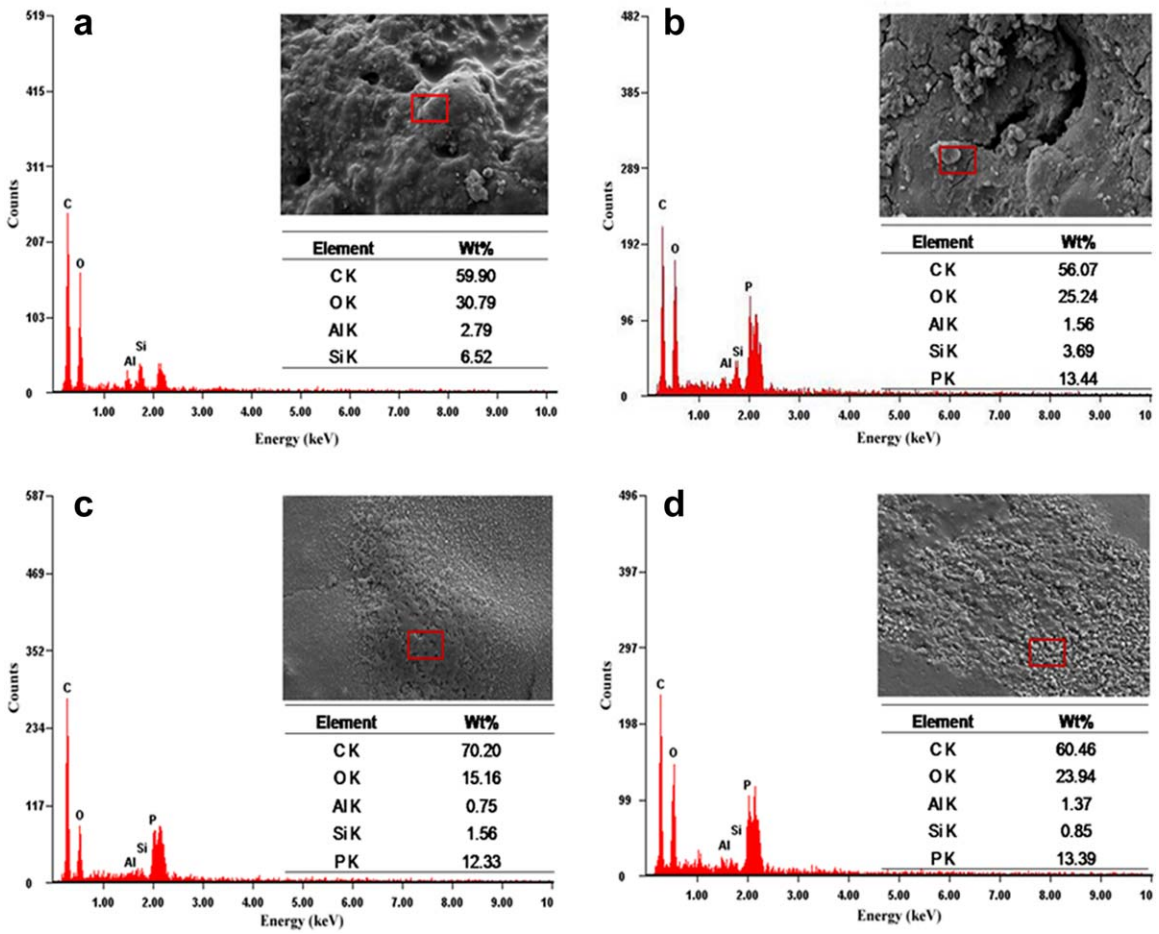


**Figure 3.** EDX spectrum showing the occurrence of elements in the char residue. (a) PLA/OMMT, (b) PLA/OMMT/FR10, (c) PLA/OMMT/FR20, and (d) PLA/OMMT/FR30. [Color figure can be viewed in the online issue, which is available at wileyonlinelibrary.com.]

self-extinguishing behavior or enable the minimum requirements of the UL-94 vertical burning test to be met.[31]

When PLA was combined with OMMT and FR, the flame retardant behavior of PLA improved significantly. The UL-94 rating of the PLA nanocomposites improved as the FR loading increased. After adding 10 phr of FR to the PLA, the mean total after-flame time after two cycles of flame exposure was greatly reduced (7.2 s). Because the flaming drips still occurred during the test, the PLA/OMMT/FR10 was assigned a V-2 rating. At higher FR loadings (i.e., 20 phr and 30 phr), a slight change in flame resistance was observed: the falling drips did not ignite the cotton indicator. Specifically, the dripping FR-containing PLA will not lead to a fire accident. The after-flame time for each flame application to the 20 phr and 30 phr FR loaded material were approximately 3.1 seconds and 1.4 s, respectively, leading to V-0 ratings.

Bourbigot and Le Bras[22] reported that organophosphorus compounds could work efficiently in oxygen-containing polymers. Therefore, FR should enhance the flame resistance of PLA. The varied efficiency of phosphorus compounds in different polymers is related to their susceptibility toward dehydration and char formation. The interaction between phosphorus flame retardants and polymers without hydroxy groups is slow and must be preceded by an oxidation. Green[32] reported that phosphorus-based flame retardants can function in the condensed phase, the gas phase, or concurrently in both phases. The phosphorus compounds are important for hindering flames in the condensed phase when used in oxygenated and hydroxylated organic polymers.

According to Dombrowski,[33] organophosphorus compounds decompose to form phosphorus-based oxides and acids in the condensed phase during thermal decomposition. The phosphoric acid acts as a catalyst, esterifying and dehydrating the polymer matrix. Subsequently, a copious char is formed, insulating the polymer substrate from heat, flame and oxygen. The phosphoric acid also acts as a physical barrier against the volatilization of fuel from the hydrocarbon polymer protected by triphenyl phosphates.[34] Concurrently, water and non-combustible gas are generated from the decomposition of the phosphate esters. This water may act as a coolant, while the non-combustible gas dilutes the active oxygen concentration and slows decomposition.[35]

### Morphological Analysis

The char residues remaining after the UL-94 vertical burning test were investigated via FESEM. The analysis was performed to study the effect of char formation on the combustion of the

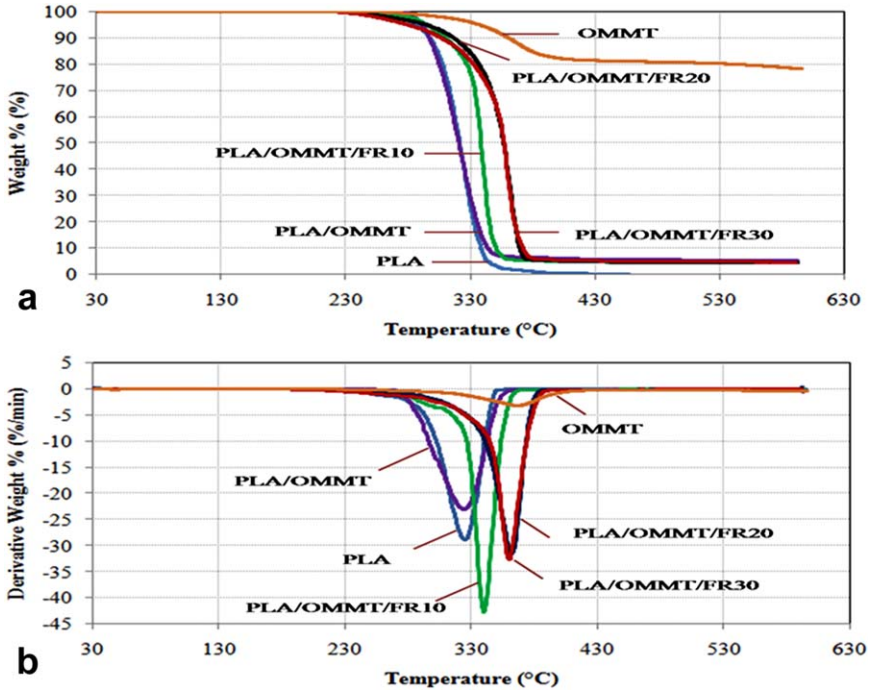


**Figure 4.** (a) TGA curves and (b) DTG curves of PLA nanocomposites with different FR loadings under nitrogen. [Color figure can be viewed in the online issue, which is available at wileyonlinelibrary.com.]

flame-resistant PLA nanocomposites. Figure 2 shows the char morphologies of PLA/OMMT and PLA/OMMT/FR. Generally, polymer charring involves various stages, such as cross-linking, aromatization, fusion of aromatics, and graphitization. The ability of a polymer to form char depends primarily on the polymeric structure. Char is formed only if the cross-linked polymer contains aromatic fragments or conjugated double bonds that are prone to aromatization during thermal decomposition.[26] PLA does not undergo char formation stages when subjected to fire. Therefore, smooth surfaces without char formation were observed after burning the PLA. The vigorous bubbling of the burning PLA forms several pores on the surface of the specimen.

After incorporating 5 wt % OMMT, a slight change in the morphology of the char residues was observed. Based on the observations in Figure 2b, island-like structures of char with many pores were apparent after burning PLA/OMMT. In addition, layered silicates accumulated on the sample surface. This phenomenon was mainly attributed to the transportation of the layered silicates by the numerous rising bubbles of degradation products and by the associated convection flow in the melt from the interior of the sample toward the surface.[36] Besides, Lewin[37] also suggested that lower surface free energy of clay causes the migration of clay platelets to the polymer surface.

Kashiwagi et al.[38] revealed that the formation of island-like flocculates rather than a continuous net-like protective layer is mainly due to the effect of the bursting bubbles near the specimen surface, propelling the accumulated clay particles outward. They had considered bubbling of nanocomposites during combustion as a disturbance element that reducing flame retarding effect. Therefore, the PLA/OMMT nanocomposite samples did not produce sufficient amounts of protective char to cover the

**Table III.** TGA-Derived Properties of PLA Nanocomposites with Various FR Contents

| Materials designation | Decomposition temperature (°C) | | | | | Char yield (%) at 600°C |
|---|---|---|---|---|---|---|
| | $T_o$ | $T_{10}$ | $T_{50}$ | $T_d$ | *$T_{max}$ | |
| PLA | 259.5 | 297.9 | 321.7 | 340.3 | 324.9 | 0 |
| PLA/OMMT | 274.6 | 297.5 | 320.9 | 347.3 | 324.8 | 3.99 |
| PLA/OMMT/FR10 | 235.0 | 310.4 | 338.7 | 352.6 | 340.6 | 4.57 |
| PLA/OMMT/FR20 | 227.9 | 317.4 | 357.0 | 369.7 | 362.4 | 4.46 |
| PLA/OMMT/FR30 | 223.1 | 307.5 | 357.2 | 372.7 | 360.4 | 4.75 |
| OMMT | 258.4 | 361.4 | - | 389.5 | 367.5 | 78.33 |

$T_{max}$ = Peak temperature at maximum decomposition rate. The data were obtained from DTG curves.

**Table IV.** Weight Loss of PLA Nanocomposites Determined from the TGA Curves at Different Temperatures

| | Weight loss (%) | | | | | |
|---|---|---|---|---|---|---|
| Material designation | $W_{100}$ | $W_{200}$ | $W_{300}$ | $W_{400}$ | $W_{500}$ | $W_{600}$ |
| PLA | 0 | 0 | 11.6 | 99.5 | 99.9 | 100 |
| PLA/OMMT | 0 | 0 | 12.9 | 95.3 | 95.9 | 96.0 |
| PLA/OMMT/FR10 | 0 | 0 | 6.3 | 94.9 | 95.4 | 95.4 |
| PLA/OMMT/FR20 | 0 | 0 | 5.8 | 94.8 | 95.4 | 95.5 |
| PLA/OMMT/FR30 | 0 | 0 | 8.2 | 94.4 | 95.1 | 95.2 |
| OMMT | 0 | 0 | 1.5 | 17.5 | 19.2 | 21.7 |

$W_{100}$, $W_{200}$, $W_{300}$, $W_{400}$, $W_{500}$, and $W_{600}$ indicate percentage of weight loss at 100, 200, 300, 400, 500 and 600°C, respectively.

entire sample surface. In addition, porous char layers possess numerous channels and apertures, allowing gas and molten polymer to overflow and enter the flame region; these layers were unable to protect the polymer from the heat of the flame,[39] possibly explaining the "no rating" from the UL-94 vertical burning test.

For systems containing FR, the morphology of the residues considerably improved. For the PLA/OMMT/FR10 residue, the char was discontinuous but still cohesive compared to the PLA/OMMT. Figure 2c also reveals that the char was not sufficiently compact, leaving the polymer matrix highly exposed. Concurrently, the matrix of the PLA/OMMT/FR10 cracked, leaving a pathway for the rapid release of combustion gases into flame and enabling access to oxygen from the atmosphere; therefore, the char layer could not provide fire protection, explaining why the UL-94 vertical burning test rankings were not as high as those for the other PLA/OMMT materials with flame retardants.

When 20 phr and 30 phr of FR were present in the PLA/OMMT nanocomposites, a drastic change in char morphology was observed: homogeneous char that was strongly adhered to the underlying composites was formed (c.f. Figure 2d and Figure 2e). According to Mouritz and Gibson,[40] the strong adhesion of the char to the polymer surface is critical to ensure that the char will not flake off and expose the virgin material to the fire. PLA nanocomposites with 20 phr and 30 phr FR had exhibited a compact, coherent and continuous char morphology that sufficiently covered and shielded the PLA matrix from the fire. Surprisingly, few or no matrix cracks and pores could be observed on the surface char of the PLA/OMMT/FR20 and PLA/OMMT/FR30. The char formed on these structures could reduce the heat and mass transfer to the underlying material and limit access to the atmospheric oxygen, slowing the decomposition rate of the polymer matrix.

Phosphorus-containing flame retardants have char forming characteristics on those polymers with oxygen or nitrogen in their structure.[41] The char forming action is often endothermic (at least in its earlier stage) and water-releasing, contributing to flame extinguishment. In addition to taking up heat radiating from the flame, the released water could dilute the fuel released during the pyrolysis of the polymer. Concurrently, the nonvolatile phosphorus flame retardants coat the burning polymer with phosphoric and polyphosphoric acid, simultaneously forming a carbonaceous layer with a glassy coating. The protective layer is resistant to high temperatures, shielding the underlying polymer from oxygen and radiant heat.[42]

To understand the occurrence of elements in the char residue of the PLA nanocomposites, the char residues from the UL-94 vertical burning test were analyzed using EDX, showing that carbon, oxygen, aluminum and silicon elements were present on the char layer surface (c.f. Figure 3a). The Al and Si traces are attributed to the OMMT because the smectite OMMT has a basic structure that includes an octahedral aluminum sheet between two tetrahedral silica sheets.[43] During thermal decomposition, the OMMT collapsed to form a carbonaceous silicate char, shielding the polymer matrix by preventing heat flux and mass transfer on the remaining resin.

After adding the phosphorus flame retardant, a phosphorus trace was detected on the char layer surface for PLA/OMMT/FR10, PLA/OMMT/FR20 and PLA/OMMT/FR30 (c.f. Figure 3b, 3c and 3d). Phosphorus-based flame retardants impart flame resistance to polymers by promoting the development of a char layer on the polymer surface, forming phosphoric and related acid anhydrides that operate as dehydrating agents.

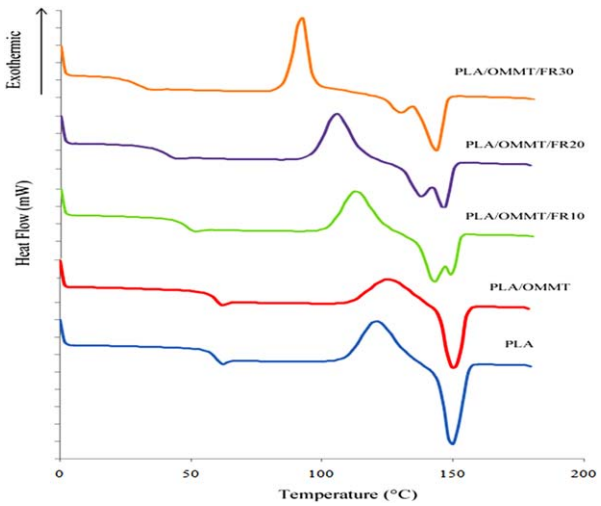


**Figure 5.** DSC thermograms of the PLA/OMMT nanocomposites. [Color figure can be viewed in the online issue, which is available at wileyonlinelibrary.com.]

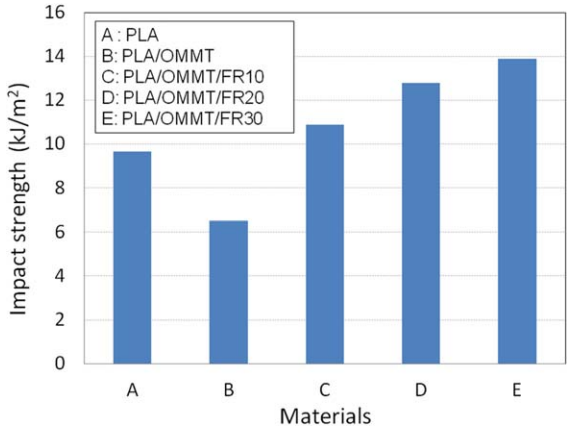


**Figure 6.** Impact strength of PLA/OMMT/FR nanocomposites. [Color figure can be viewed in the online issue, which is available at wileyonlinelibrary.com.]

During dehydration, double bonds are produced, promoting further cross-linked and carbonized structures at high temperatures. Yuan et al.[44] also reported that the phosphorus-rich residues formed during the thermal degradation could protect the underlying polymer from further decomposition. The percentage of phosphorus remaining in the residue after combustion indicates that the remaining FR in the condensed phase interrupts pyrolysis and induces char formation. Concurrently, the volatile phosphorus compounds (PO·, $PO_2$·, and HPO·) could vaporize quantitatively from the polymer surface, inhibiting flames in the gas phase via free-radical trapping. In addition, 50 to 99% of the phosphorus compounds should be evolved and lost, possibly including $P_2O_5$ or other oxides formed during pyrolysis.[22] Therefore, compact char formation was one of the important mechanisms for quenching the spread of flames and was strongly proven.

### Thermogravimetry Analysis

Figure 4a shows the TGA curves for PLA and its composites. Table III summarizes the thermal characteristics extracted from the TGA and DTG curves.

Based on Figure 4a, the thermal decomposition of samples with various flame retardant loadings occurs in one stage. All samples exhibited a similar decomposition curve, undergoing slow decomposition at lower temperatures (i.e., 230–280°C) and rapid decomposition at higher temperatures (i.e., 280–380°C). The thermal decomposition of PLA is a very complicated process that involves different mechanisms. The pristine PLA begins to decompose at approximately 259°C, losing ester groups from the main chain (cleavage of carbonyl carbon-oxygen bond). Concurrently, intra-molecular transesterification reactions occur, forming cyclic lactic acid and lactide oligomers. Simultaneously, the cyclic oligomers recombine with the linear polyesters via insertion to form longer macromolecular chains. During decomposition, cyclic oligomers, lactide, acetaldehyde, carbon monoxide and carbon dioxide are released as gaseous products. The pristine PLA starts to decompose at 259.5°C and fully decomposed at 600°C. Figure 4b reveals that the maximum decomposition rate for PLA occurs at 325°C.

**Table V.** DSC Thermal Characteristics of the PLA/OMMT Nanocomposites

| | Thermal characteristics | | | |
|---|---|---|---|---|
| Materials designation | $T_g$ (°C) | $T_{cc}$ (°C) | $T_{m1}$ (°C) | $T_{m2}$ (°C) |
| PLA | 59.5 | 120.7 | 149.5 | – |
| PLA/OMMT | 59.6 | 126.0 | 150.9 | – |
| PLA/OMMT/FR10 | 47.7 | 112.3 | 149.3 | 141.8 |
| PLA/OMMT/FR20 | 41.3 | 105.5 | 146.8 | 137.1 |
| PLA/OMMT/FR30 | 29.9 | 91.2 | 142.6 | 128.3 |

The thermal stability of PLA is improved by adding 5 wt % OMMT (c.f. Table III). The OMMT increases the onset ($T_o$) and end decomposition temperatures ($T_d$) of neat PLA by 15°C and 7°C, respectively. The decomposition of OMMT started at 258.4°C, with a total mass loss of 21.67°C. Compared to the pristine PLA without residual char, the PLA/OMMT nanocomposite yields 3.99 wt % char after the experiment. Similar observations were reported by Kontou et al.[45] and Wang et al.[46] This behavior is mainly due to the physical and chemical reactions promoted by OMMT during decomposition. The clay collapses to form a clay-rich barrier, hindering the out-diffusion of volatile decomposition products and slowing the pyrolysis of the decomposing polymer. Moreover, MMT layered silicates can function as a heat barrier, resisting heat transfer and facilitating char formation during thermal decomposition.[47] The improved overall thermal stability for the polymer nanocomposites is attributed to the ablative reassembling of the silicate layers functioning as a physical protective barrier.

An interesting phenomenon has been observed when PLA nanocomposites containing different loadings of FR undergo thermal decomposition. Based on Figure 4a, the $T_o$ of all of the PLA/OMMT/FR composites are obviously lower than that of neat PLA due to the decomposition of the FR. The Reofos 50 FR undergoes a 5% weight loss at 216°C, a 10% weight loss at 235°C, a 50% weight loss at 284°C and loses almost all of its mass by 340°C.[48] The higher the FR content of the PLA/OMMT composites, the lower the $T_o$ detected during TGA is. The $T_o$ of the pristine PLA shifted toward lower temperatures by 24.5°C, 31.6°C and 36.4°C for PLA/OMMT/FR10, PLA/OMMT/FR20, and PLA/OMMT/FR30, respectively. Surprisingly, the temperatures at 10% weight loss ($T_{10}$), 50% weight loss ($T_{50}$), and the end of decomposition ($T_d$) are significantly increased after adding FR (c.f. Table III), implying that FR can stabilize and delay any further decomposition in the PLA/OMMT nanocomposites.

According to Zuo et al.,[49] the $T_o$ must shift toward lower temperatures for PLA nanocomposites with flame retardants when compared to pure PLA because the phosphorus-containing flame retardant must decompose at the beginning of combustion to form phosphoric and polyphosphoric acids. These acids accelerate the esterification and carbonization reactions that help form char, protecting the polymer from continued heat

degradation. The stabilization effect by FR dominates the degradation process after the FR thermally decomposes, delaying weight loss for the PLA/OMMT and increasing the $T_{10}$, $T_{50}$, and $T_d$. These acids can form a molten viscous surface layer, protecting the underlying polymer from flames and oxygen.[50]

Moreover, the residual char yield of the PLA/OMMT/FR nanocomposites increases with the FR content. Table III reveals that the char left at the end of experiment totals 4.57 wt %, 4.46 wt % and 4.75 wt % for PLA/OMMT/FR10, PLA/OMMT/FR20 and PLA/OMMT/FR30, respectively, exceeding the contents for the neat PLA and PLA/OMMT nanocomposite. Therefore, FR promotes char formation at higher temperatures. The increased formation of carbonaceous material during combustion improves the flame-retardant behavior and thermal stability during the late stages of degradation. However, the phosphorus compounds resist combustion by forming a layer of char, inhibiting carbon monoxide and carbon dioxide formation and reducing the amount of heat supplied to the system. According to Lin et al.,[51] when a phosphorus-based flame retardant has decomposed and released phosphoric acid, these acids react with the hydroxyl groups in the polymer, and the resulting polyol polymer decomposes to form char. However, there is too little char residue after the experiment compared to other systems containing flame retardant, indicating that PLA was not a good carbonization agent because too few hydroxyl groups were present in the neat PLA.

Figure 4b displays the DTG curves of the PLA nanocomposites under nitrogen. The single peak in the DTG curves reveals that complete thermal degradation occurs in one step. Adding OMMT to PLA does not change the magnitude of the DTG peak transition, although OMMT has a higher $T_{max}$ value (i.e., 367.5°C). The $T_{max}$ of PLA and PLA/OMMT are similar (i.e., 324.9°C and 324.8°C), while the DTG peak of PLA/OMMT is lower than that of PLA. Therefore, the inclusion of OMMT lowered the weight loss rate and enhanced the thermal stability of neat PLA. The clay layers act as physical barriers, restricting the mobility of macromolecules and the escape of the decomposition products.

When FR is present in the PLA/OMMT nanocomposite, a peak shifting pattern has been observed. The DTG peaks are shifted toward higher temperatures, generating a higher $T_{max}$. The $T_{max}$ of the PLA is increased by 15.7°C, 37.5°C, and 35.5°C after adding 10 phr, 20 phr, and 30 phr of FR, respectively. As the FR content increases, the $T_{max}$ are shifted toward higher temperatures, indicating that the phosphorus-based flame retardant delays the mass loss rate by enhancing the production of a protective surface layer of char, inhibiting access to oxygen and escape of carbon oxides via physical blockage. Concurrently, the phosphorus-based flame retardant interrupts the oxidation reaction of carbon to carbon monoxide and carbon dioxide. However, the PLA/OMMT nanocomposites containing FR exhibit higher peaks than neat PLA or PLA/OMMT, particularly PLA/OMMT/FR10. Therefore, the weight loss rate increased after introducing the FR; the decomposition of the phosphorus flame retardant yields phosphoric and polyphosphoric acids in the condensed phase, accelerating the thermal degradation and chain stripping in the PLA. This result agrees with the observations reported by Elakesh et al.,[48] indicating that introducing Reofos 50 FR to chlorinated poly(vinyl chloride) tends to promotes dehydrochlorination and chain stripping via phosphoric acid release. In addition, the height of the DTG peaks decreases as the FR loadings into PLA/OMMT nanocomposites increase, indicating that higher FR loadings can suppress weight loss rate and improve the thermal stability of the PLA nanocomposites.

Table IV shows the weight loss of PLA nanocomposites determined from the TGA curves at different temperatures. Based on Table IV, we can notice that all the samples having their single mass loss process around temperature 220 to 390°C. At the beginning of thermal decomposition, PLA/OMMT displays higher mass loss compare to pristine PLA and PLA/OMMT/FR composites. This is mainly attributed to decomposition of organic intercalant of the OMMT, which further leads to formation of clay-rich barrier that slowing down the decomposition of PLA. As result, the mass loss rate of PLA/OMMT has reduced at temperature after 400°C. In the present of FR, PLA/OMMT composites have relatively low mass loss at the beginning of thermal decomposition. PLA/OMMT/FR30 exhibits highest mass loss, following by PLA/OMMT/FR10 and PLA/OMMT/FR20. Recall that the FR having lower onset decomposition temperature tends to decompose in the beginning of combustion. The formation of phosphoric and polyphosphoric acids accelerate the esterification and carbonization reaction to form char, protecting the polymer from continued thermal degradation.

### Differential Scanning Calorimetry

Based on the Figure 5, it can be obviously seen that the neat PLA and PLA/OMMT exhibit similar thermal events, for instance glass transition, cold crystallization and single melting peak. In this study, the $T_g$ and $T_m$ of pristine PLA are found to be 59.5°C and 149.5°C, respectively. The introduction of OMMT does not give any significant influence on the $T_g$ of PLA, indicating that the present of OMMT did not affect the chain mobility of PLA.

An interesting trend in the thermograms has been observed for PLA/OMMT nanocomposites containing FR (c.f. Figure 5). The $T_g$ is greatly decreased from 59.6°C for PLA/OMMT to 47.7°C for PLA/OMMT/FR10, 41.3°C for PLA/OMMT/FR20 and 29.9°C for PLA/OMMT/FR30. Therefore, the higher the FR loading the lower the $T_g$ is shifted, neglecting the effect of OMMT. For every 10 phr of FR incorporated, the $T_g$ is shifted toward lower temperatures by almost 10°C. This decrease is attributed to the segmental mobility of PLA due to plasticization. Saeidlou et al.[52] has reported that increase in chain mobility able to facilitate the chains movement from the amorphous phase into the crystal surface, especially at lower temperatures. Additionally, we have conducted impact test on the PLA/OMMT/FR nanocomposites, and it was found that the impact strength of PLA/OMMT was significantly improved by the addition of FR (c.f. Figure 6).

Concurrently, the $T_{cc}$ of the PLA/OMMT/FR composites are shifted toward lower temperatures compare to PLA/OMMT.

The crystallization peaks are shifted toward lower temperatures when additional FR is added. The FR favors crystallization in the PLA by increasing the segmental mobility of the PLA chains due to plasticization. According to Li and Huneault,[53] decreased $T_{cc}$ values can be attributed to increased polymer chain mobility at low temperatures, followed by a larger depression of $T_g$. The reduced $T_g$ allows the crystallization to start at lower temperatures during heating. In addition, the presence of readily formed crystalline nuclei during the cooling process shortens the crystallization induction period. These nuclei should increase the crystallization rate during heating because the crystalline structure is more densely nucleated when the polymer is being cooled from the melt. Therefore, combining $T_g$ with a high nucleation density shifted the crystallization peaks toward lower temperatures as the FR content increased.

Regarding the melting behavior, the exothermic melting of PLA is slightly shifted toward lower temperatures in the presence of FR. Table V reveals that the melting peak shifted from 149.5°C for PLA to 149.3°C for PLA/OMMT/FR10, 146.8°C for PLA/OMMT/FR20 and 142.6°C for PLA/OMMT/FR30. As the amount of FR in PLA/OMMT increased, the melting peak shifted toward lower temperatures. According to Piorkowska et al.,[54] the formation of imperfect crystals decreases the melting temperature of the PLA crystals in the composites because the plasticizer accelerates the spherulite growth rate.

In contrast to PLA and PLA/OMMT with their single melting peaks, the PLA/OMMT/FR systems display double melting peaks from 128.3 to 149.3°C. On the DSC thermograms of PLA/OMMT/FR10, a shoulder appears on the descending slope of the melting peak at 141.8°C. For PLA/OMMT/FR20 and PLA/OMMT/FR30, a broad peak is developed at lower temperatures (137.1°C and 128.3°C, respectively) associated with the melting peak at higher temperatures. In this study, the presence of bimodal endothermic melting in the PLA/OMMT/FR nanocomposites can be related to the melt-recrystallization mechanism or polymorphism phase transition. Picard et al.[55] has revealed that each melting peak is the signature of a crystalline lamella population that essentially characterized by its thickness or its perfection. The melting peak at low temperature is due to the melting of thinner lamellar, while the melting peak at high temperature is originates from the thicker lamellar. It is also known that a low temperature melting peak is assigned to the primary crystallites formed at $T_c$, and high temperature melting peaks reflect the relatively perfect lamellar stacks resulting from recrystallization during the heating scan.

## CONCLUSIONS

Phosphorus-based flame-retardant PLA clay nanocomposites were successfully prepared using a melt compounding technique. The effects of OMMT and a phosphorus-based flame retardant (Reofos 50 FR) on the flammability and thermal properties of PLA/OMMT nanocomposites were investigated. The UL-94 vertical burning test revealed that neat PLA burned with flaming drips and bubbling after the flame was applied. The presence of OMMT suppressed the dripping but could not impart a self-extinguishing characteristic. The flame resistance of PLA was significantly enhanced by the inclusion of FR. The rating of PLA was improved from V-2 to V-0 after adding 20 phr and 30 phr of FR. For the char morphology, no char was formed on the surface of the neat PLA specimen because PLA did not undergo char formation stages. The amount of char formed by OMMT on the surface of the specimen could not cover or protect the entire sample surface. To form a compact, coherent and continuous protective char layer, at least 20 phr of FR is required in the PLA/OMMT nanocomposites. The char morphology detected via FESEM and EDX further elucidated the existence of the condensed phase mechanism while quenching and retarding flame propagation. From the TGA results, PLA undergoes a single-step thermal degradation and begins to decompose at 260°C. OMMT functions as a physical protective barrier, hindering the outward diffusion of volatile decomposition products and resisting heat transfer during decomposition to enhance the thermal stability of PLA. Adding FR to the PLA/OMMT nanocomposites has affected the thermal stability. FR is readily decomposed at the beginning of combustion to yield phosphoric and polyphosphoric acids that induce char formation in the condensed phase. The carbonaceous char should insulate the polymer substrate from heat, flame and oxygen. The stabilization and delay of decomposition was more apparent in the PLA/OMMT/FR20 and PLA/OMMT/FR30. Additionally, the FR shifted the $T_g$, $T_{cc}$ and $T_m$ of PLA/OMMT composites toward lower temperatures. FR could induce plasticization on PLA/OMMT. The impact strength of PLA/OMMT was increased by the addition of FR. In summary, flexible PLA nanocomposites with high flame resistance were successfully produced.

## ACKNOWLEDGMENTS

This study was funded by a Universiti Sains Malaysia Research University Grant (grant numbers 814070 and 814199), a Fundamental Research Grant Scheme (Ministry of Higher Education, Malaysia; grant number 6071260), and a USM Incentive Grant (grant number 8021013).

## REFERENCES

1. Auras, R.; Harte, B.; Selke, S. *Macromol. Biosci.* **2004**, *4*, 835.
2. Qi, R.R.; Luo, M.N.; Huang, M. *J. Appl. Polym. Sci.* **2011**, *120*, 2699.
3. Dong, W.F.; Zou, B.S.; Ma, P.M.; Liu, W.C.; Zhou, X.; Shi, D.J.; Ni, Z.B.; Chen, M.Q. *Polym. Int.* **2013**, *62*, 1783.
4. Li, S.; Yuan, H.; Yu, T.; Yuan, W.; Ren, J. *Polym. Adv. Technol.* **2009**, *20*, 1114.
5. Chow, W.S.; Lok, S.K. *Polym. Polym. Comp.* **2008**, *16*, 263.
6. Morgan, A.B. *Polym. Adv. Technol.* **2006**, *17*, 206.
7. Leu, Y.Y.; Mohd Ishak, Z.A.; Chow, W.S. *J. Appl. Polym. Sci.* **2011**, *124*, 1200.
8. Pluta, M. *Polymer* **2008**, *45*, 8239.
9. Murariu, M.; Ferreira, A.D.S.; Alexandre, M.; Dubois, P. *Polym. Adv. Technol.* **2008**, *19*, 636.
10. Choi, K.; Choi, M.; Han, D.; Park, T.; Ha, C. *Eur. Polym. J.* **2013**, *49*, 2356.

11. Paul, M. A.; Alexandre, M.; Degée, P.; Henrist, C.; Rulmont, A.; Dubois, P. *Polymer* **2003**, *44*, 443.
12. Chow, W. S.; Leu, Y. Y.; Mohd Ishak, Z. A. *J. Comp. Mater.* **2014**, *48*, 155.
13. Balakrishnan, H.; Hassan, A.; Wahit, M. U.; Yussuf, A.A. *Mater. Des.* **2010**, *31*, 3289.
14. Jung, C. H.; Hwang, I. T.; Jung, C. H.; Choi, J. K. *Radiat. Phys. Chem.* **2014**, *102*, 23.
15. Meng, B.; Tao, J.; Deng, J. J.; Wu, Z. H.; Yang, M. B. *Mater. Lett.* **2011**, *65*, 729.
16. Zhao, Q.N.; Ding, Y.; Yang, B.; Ning, N.Y.; Fu, Q. *Polym. Test.* **2013**, *32*, 299.
17. Bourbigot, S.; Fontaine, G. *Polym. Chem.* **2010**, *1*, 1413.
18. Janssen, S. Brominated Flame Retardants: Rising Levels of Concern, Health Care Without Harm (HCWH) Publisher: USA, **2005**.
19. Davis, J.; Huggard, M. *J. Vinyl. Addict. Technol.* **1996**, *2*, 69.
20. Dufton, P.W. Flame Retardants for Plastics Market Report, Rapra Technology Limited: UK, **2003**.
21. Green, J. *J. Fire Sci.* **1996**, *14*, 353.
22. Bourbigot, S.; Le Bras, M. In Plastics Flammability Handbook: Principles, Regulations, Testing and Approval, 3rd ed.; Troitzsch, J., Ed.; Hanser Publishers: Munich, **2004**; p 133.
23. Wei, L. L.; Wang, D. Y.; Chen, H. B.; Chen, L.; Wang, X. L.; Wang, Y. Z. *Polym. Degrad. Stab.* **2011**, *96*, 1557.
24. Wang, D. Y.; Song, Y. P.; Lin, L.; Wang, X. L.; Wang, Y. Z. *Polymer* **2011**, *52*, 233.
25. Flint, A. J., Jr. In The Basics of Testing Plastics: Mechanical Properties, Flame Exposures and General Guidelines; Driscoll S. B., Ed.; Mayfield: ASTM, **1998**; p 53.
26. Levchik, S.V. In Flame Retardant Polymer Nanocomposites; Morgan, A. B.; Wilkie, C. A., Eds.; John Wiley and Son: USA, **2007**; p 19.
27. Hirschler, M. M. In Fire Retardancy of Polymeric Materials; Grand, A. F.; Wilkie, C. A., Eds.; Marcel Dekker: New York, **2000**; p 81.
28. Kiliaris, P.; Papaspyrides, C. D. *Prog. Polym. Sci.* **2010**, *35*, 902.
29. Anna, P.; Matkó, S.; Marosi, G.; Nagy, G.; Alméras, X.; Le Bras, M. In Fire Retardancy of Polymers: New Applications of Mineral Fillers; Le Bras, M.; Bourbigot, S.; Duquesne, S.; Jama, C.; Wilkie, C.A., Eds.; RSC Publishing: Cambridge, **2005**; p 336.
30. Nazare, S.; Hull, T. R.; Biswas, B.; Samyn, F.; Bourbigot, S.; Jama, C.; Castrovinci, A.; Fina, A. In Fire Retardancy of Polymers: New Strategies and Mechanisms; Hull, T. R.; Kandola, B. K., Eds.; Royal Society of Chemistry: Cambridge, **2009**; p 168.
31. Cheng, K. C.; Yu, C. B.; Guo, W.; Wang, S. F.; Chuang, T. H.; Lin, Y. H. *Carbohydr. Polym.* **2012**, *87*, 1119.
32. Green, J. *J. Fire Sci.* **1992**, *10*, 470.
33. Dombrowski, R. *J. Coat Fabr.* **1996**, *25*, 224.
34. Lewin, M.; Weil, E.D. In Fire Retardant Materials; Horrocks, A. R.; Price, D., Eds.; Woodhead Publishing Limited: Cambridge, **2000**; p 31.
35. Fire, F. L. Combustibility of Plastics, Van Nostrand Reinhold: USA, **1991**.
36. Qin, H.; Zhang, S.; Zhao, C.; Hu, G.; Yang, M. *Polymer* **2005**, *46*, 8386.
37. Lewin, M. *Fire Mater.* **2003**, *27*, 1.
38. Kashiwagi, T.; Harris, R. H. J.; Zhang, X.; Briber, R. M.; Cipriano, B. H.; Raghavan, S. R.; Awad, W. H.; Shields, J. R. *Polymer* **2004**, *45*, 881.
39. Zhang, R.; Xiao, X.; Tai, Q.; Huang, H.; Yang, J.; Hu, Y. *J. Appl. Polym. Sci.* **2012**, *127*, 4967.
40. Mouritz, A.P.; Gibson, A.G. Fire Properties of Polymer Composite Materials, Springer: Netherlands, **2006**.
41. Weil, E.D.; Levchik, S.V. Flame Retardants for Plastics and Textiles: Practical Applications, Carl Hanser Verlag: Germany, **2009**.
42. Troitzsch, J. In International Plastics Flammability Handbook: Principles, Regulations, Testing and Approval, 2nd ed.; Troitzsch, J., Ed.; Carl Hanser Verlag: Germany, **1990**; p 43.
43. Chow, W. S.; Mohd Ishak, Z. A.; Karger-Kocsis, J.; Apostolov, A. A.; Ishiaku, U. S. *Polymer* **2003**, *44*, 74270.
44. Yuan, X.; Wang, D.; Chen, L.; Wang, X.; Wang, Y. *Polym. Degrad. Stab.* **2011**, *96*, 1669.
45. Kontou, E.; Niaounakis, M.; Georgiopoulos, P. *J. Appl. Polym. Sci.* **2011**, *122*, 1519.
46. Wang, B.; Wan, T.; Zeng, W. *J. Appl. Polym. Sci.* **2012**, *125*, 364.
47. Chow, W. S.; Lok, S. K. *J. Therm. Anal. Calorim.* **2009**, *95*, 627.
48. Elakesh, E. O.; Hull, T. R.; Price, D.; Milnes, G. J.; Carty, P. *J. Vinyl. Add. Technol.* **2005**, *11*, 21.
49. Zuo, J.; Su, Y.; Liu, S.; Sheng, Q. *J. Polym. Res.* **2011**, *18*, 1125.
50. Green, J. In Fire Retardancy of Polymeric Materials; Grand, A. F.; Wilkie, C. A., Eds.; Marcel Dekker: New York, **2000**; p 147.
51. Lin, H.; Liu, S.; Han, L.; Wang, X.; Bian, Y.; Dong, L. *Polym. Degrad. Stab.* **2013**, *98*, 1389.
52. Saeidlou, S.; Huneault, M.A.; Li, H.; Park, C. B. *Progr. Polym. Sci.* **2012**, *37*, 1657.
53. Li, H.; Huneault, M. A. *Polymer* **2007**, *48*, 6855.
54. Piorkowska, E.; Kulinski, Z.; Galeski, A.; Masirek, R. *Polymer* **2006**, *47*, 7178.
55. Picard, E.; Espuche, E.; Fulchiron, R. *Appl. Clay Sci.* **2011**, *53*, 58.